Energy 239 (2022) 122332

Contents lists available at ScienceDirect

Energy

journal homepage: www.elsevier.com/locate/energy

Comprehensive solar thermal integration for industrial processes

Guillermo Martínez-Rodríguez*, Amanda L. Fuentes-Silva, Daniel Velázquez-Torres, Martín Picón-Núñez

Department of Chemical Engineering, University of Guanajuato, Guanajuato, 36050, Mexico

ARTICLE INFO

Article history:
Received 8 January 2021
Received in revised form
29 August 2021
Accepted 11 October 2021
Available online 14 October 2021

Keywords:
Solar thermal integration
Solar thermal minimum temperature difference
Zero emissions
Cost of the solar thermal energy
Solar fraction

ABSTRACT

The thermal integration into industrial process is majorly focused on guarantee the heat duty and temperature level demanded by the process. Other important objectives must be considered when is integrated solar thermal energy, since its integration into industrial processes seeks to maximise its use. The present work proposes a comprehensive integration of solar thermal energy, which is based on the Pinch Analysis, and considers economical evaluation, environmental impact and the ΔT_{min}. The ΔT_{min} used to get the objectives of the solar thermal integration is denominated $\Delta T_{min,\ th}$. The approach supposes the establishment of multiple objectives before the solar system final design. Profitable costs for two case studies, dairy and 2G bioethanol processes, were obtained. For all the scenarios, the integrated solar thermal system of dairy process was viable with zero emissions of CO_2. In 2G bioethanol process, only in one scenario the solar fraction was equal to one. It is possible to reach a surplus energy of 44%, with the same absorber area of solar energy, or would be possible to reduce the area by 49% to supply the heat duties.

1. Introduction

Global energy consumption in the industrial sector is significant, only the process heat consumes 74% of the total industrial energy demand and more than 50% of the industrial heating demand is in the temperature range between 60 and 250 $^{\circ}C$ [1]. Currently, only 9% of the demand for industrial process heat is supplied from renewable energy sources [2], with 741 industrial plants that use solar heat with a total area of solar collectors of 662,648 m^2(567 $MWth$), that were reported in 2019 [3]. Applications of solar thermal energy (STE) in industry lead to sustainable production [4].

Solar thermal energy integration to industrial processes implies the study and knowledge of relevant issues: solar potential, current state of technology, methods and extensions of solar heat integration, performance evaluation of solar thermal equipment, economic and environmental evaluation, barriers to large-scale adoption, costs, and the most representative case studies in literature [5]. Pinch Methodology has been successfully extended to solidly support the integration of solar energy into industrial processes, and to comply with regulations or environmental policies, limits on the total cost, decrease or elimination of GHG emissions, among others [6]. Atkins et al. [7] established is central that solar thermal system provides heat above the Pinch point; so, the integration be efficient, and savings are achieved in both, hot and cold utilities.

The STE that is captured by a solar collector network (SCN) can be considered a solar utility [8]. STE integration allows to achieve operation objectives that favour the achievement of environmental objectives. Quijera et al. [9] used Pinch Analysis to reduce the use of fossil fuels by 11.4%, considering not limited surface for the installation of solar collectors, in a tuna canning process which operates in batches, in a region where diffuse radiation predominates over direct radiation. Eiholzer et al. [10] found that solar heat can only account for a maximum of 7.7% of heat demand for a brewery operating in batches due to the restrictions of UK incentive program, however the study showed that this value could double up to 13.6%.

When the main interest was to deploy solar technology to the maximum, Baniassadi et al. [11] developed a procedure to find a better energy integration scenario, using Pinch Analysis, setting the solar fraction as an objective. They carried out an economic optimisation of the integration by calculating solar fraction for a certain amount of capital investment, however, payback time is predicted for a minimum of 7 years. At same year, Walmsley et al. [12] studied three scenarios for integration of solar energy into an industrial

* Corresponding author. Col. Noria Alta s/n, Guanajuato, Gto. CP, 36050, Mexico
E-mail address: guimarod@ugto.mx (G. Martínez-Rodríguez).

https://doi.org/10.1016/j.energy.2021.122332
0360-5442/

process using a Heat Recovery Loop (HRL) and determined that a series configuration was the best scenario for integration of solar energy; authors set ΔT_{min} at 5 °C, this value was also validated by authors in base of their own observations in the dairy plant [12]. Abdelhady et al. [13] developed a hierarchical design approach for the optimal integration of heating and power processes, achieving integration between thermal demand of the process, solar energy obtained and an auxiliary heating service. Eiholzer et al. [10] presented a method based on Pinch Analysis to optimise direct heat recovery from a batch process in a brewery, followed by integration of a solar thermal system at a chosen point. Allouhi et al. [14] presented a procedure for the optimisation and simulation of a centralised solar heating system that provides hot water to four processes with different temperature levels and load profiles. They evaluated a milk processing company as a case study and used the life cycle cost method to select the optimal size of the main design parameters for decision making. Velázquez-Torres [15] made a study of Pinch Analysis concepts and integrated low-temperature STE into a 2G bioethanol production process and determined the SCN and the thermal storage system with a smaller size and cost.

Total cost of solar thermal integration defines the viability of the installation and includes the SCN, heat recovery network, utility system and thermal storage system. Size of SCN must be evaluated in detail since it represents up to 54% of total cost of the solar thermal system [16]. Designing the collector network represents a design space that has already been evaluated by Martínez-Rodríguez et al. [17] who determined how the supply temperature to the collector network and the supply flow reduce the number of collectors in series and the number of series connected in parallel. Storage unit can improve the performance of the facility by eliminating fluctuations in energy supply [12], because its use allows guaranteeing the supply of thermal load at temperature level required by the process, and thus increasing supply time [18]. This variable represents from 11% to 30% of the total cost of solar thermal device [18].

Levelised cost of thermal energy (LCOEth) for industrial heating of solar thermal systems is determined in the range of 5–9 US cents per *kWh* with a strong sensitivity towards collector price, collector efficiency and financial parameters in each country [19]. Tian et al. [20] studied that the lowest levelised net cost of STE from hybrid solar heating plants could reach approximately 0.058 *USD*/ *kWh*. Ghazouani et al. [21] found that renewable energy utilisation rate could be higher than 40% with a cost of less than 0.05 *USD*/ *kWh* for a small thermal storage capacity; this could constitute more than 85% and cost less than 0.2 *USD*/*kWh*, implementing large thermal storage capacities.

In the complete panorama of integration, ecological footprint [22] evaluates the complete life cycle of the components of a process. One of the studies carried out on this topic [23] compared two technologies for domestic use for water heating; a result showed that flat plate thermosyphon unit systems, are less environmentally friendly, compared to their integrated collector storage counterparts. Transition towards the use of alternative sources of energy in industry, using utility systems with fossil fuels as backup, is a common scenario reported in some works, however, current primary approach, regarding the use of solar energy, is the development of methods that make possible to achieve the global goal of zero carbon emissions using 100% renewable systems, or net zero emissions, if low carbon fuel is used as backup. In this sense, some studies are already reported for electricity [24] and domestic sector (water heating and comfort) [25].

In general, the literature contains relevant research reports on the integration of STE in industrial processes and they analyse one or some variables and evaluate the objectives achieved. However, until now, there is no research that analyses how multiple variables, in a comprehensive approach, affect the objectives set in solar thermal integration, and how these variables are related to each other, giving valuable and reliable information for decision-making.

This work develops an approach for the detailed integration of STE into industrial processes to:

- impact on one or more of the following design objectives, simultaneously: solar fraction, installation area of SCN, payback time, maximum supply time, reduction in network size.
- generation of energy surpluses, for a fixed collector network size, to develop multiple utilities targeting (generating multiple utility levels [26])
- to promote processes with zero carbon emissions.
- be adapted to different scenarios, depending on the process requirements and the particular interest of the industrial engineer.
- be extended to generate cooling and power.
- be extended for medium temperature technology (medium-temperature SCN).

2. Solar thermal energy integration method

Among the various methods for the integration of processes, such as graphic methods, numerical programming methods and hybrid-type approximations, is the Pinch Analysis which allows to establish *a priori* design valuable objectives in the process. Pinch Analysis, through Process Integration improves heat recovery in the industry. This concept has been extended to integrate STE. The integrated amount of STE is related to both the captured STE and to the net process heating demands of the considered system [8].

It is viable to carry out a comprehensive integration intensifying the use of STE in industrial process. The main objective is supplying a larger amount of the hot utility demanded by a process (maximise). A detailed STE integration to process is important to maximise its use and to identify, *a priori*, the objectives from process data and integration variables. Various of those objectives have been studied in a painstaking way, as well as, it has been evaluated the impacts and results from the STE integration to an industrial process. As an example, when the interest is to reduce the size of SCN and storage system, inlet temperature, operation flow and radiation has been evaluated [18]. A comparative study between two different technologies of solar collectors, flat-plate against evacuated-tube, showed greater efficiency in these last, with a payback time of 5 months [10]. Budak et al. [27] determined the thermal efficiency of a flat-plate solar collector rise from 73 to 87% using a CuO/Water solution (0.2–0.8% w/v).

The integration of STE, proposed in this work, seeks correspondence on the temperature levels between STE and process heating demands. A thermal storage system solves the match between the times of the energy requirement by the process, and the availability times at the target temperature level of the STE. The implementation of storage seeks certainty and stability; guarantees the supply of the thermal load (at the target temperature) in the required time; and increases the supply time, of STE, when the solar resource is not available in the conditions required to reach the target temperature of the process.

Detailed STE integration lets a global vision about the involved objectives and variables. This method considers variables with prominent influence in the solar thermal integration to reach the final multi-objective design. This study determines the relationship between the different variables among themselves and evaluates the impacts on the objectives of the final solution. Fig. 1 is a general schematic about the STE integration to an industrial process, as is proposed by the authors of this paper. The main components of this proposal are next: the objectives established *a priori* (before the design), the intrinsic variables of the components of the method, and the solution, which contains the final design that meets the objectives set.

As previously stated, the objectives of the integration of STE are set prior to the final integrated solar system design. Based on process data it is possible to know the refrigeration, the power and thermal energy demands. The focus is supply thermal energy using the solar thermal source only. The minimum utilities are calculated from the process data; equally, are calculated the solar fraction and the heat recovery network associated with ΔT_{min}. Composite Curve (CC) and the Grand Composite Curve (GCC) let establish the relations between minimum hot utility and the size of SCN. The point is to supply the total hot utility with solar utility analyzing for different ΔT_{min}.

A range of ΔT_{min} of 10–30 $°C$ is recommended for the chemical and refining industry, and a ΔT_{min} of 3–5 $°C$ is recommended in the food industry [28], therefore the range used was from 5 $°C$ up to 25 $°C$. Behaviour of GCC is analysed in a range of ΔT_{min}. In this paper, a ΔT_{min} that allows achieving the objectives set when carrying out solar thermal integration is denoted as $\Delta T_{min,\ th}$.

The GCC allows maximise the use of STE, because locates the scenarios where it is possible to provide the total heat duty with that source of energy. When solar fraction has a value of one ($f = 1$), the resultant scenarios can keep the original area (size) of the SCN. The latter gives a surplus of energy to supply heat duty below the maximum temperature level reported by the CC. Otherwise, it is possible to reduce the size of the network and increase the delivery time.

2.1. Estimation of heat recovery network and SCN areas

The calculus of the areas and the auxiliary services is carried out from the CC. Heat recovery network area is calculated prior to design of the network. To design a heat exchanger Eq. (1) is applied in each section based on the assumption of “vertical” heat exchange.

$$Q = UA\Delta T_{LMTD} \tag{1}$$

where Q is thermal load (kW), U is the heat transfer global coefficient ($kW/m^2\,°C$), ΔT_{LMTD} is logarithmic mean temperature difference ($°C$). If values of the individual heat transfer coefficients are known, then the equation that predicts the necessary heat exchange area is given by Eq. (2), Bath's formula, for estimating minimum area for the synthesis of heat exchange networks [29].

$$A_k = \frac{1}{\Delta T_{LMTDk}}\left(\sum_{i}^{hot\ streams}\frac{Q_i}{h_i} + \sum_{j}^{cold\ streams}\frac{Q_j}{h_j}\right) \tag{2}$$

where A_k is the area of each interval (m^2), Q_i and $Q_j$are thermal loads from hot and cold streams (kW), h_i and h_j are the individual coefficients of hot and cold streams that exchange heat in the interval ($kW/m^2\,°C$), the estimate of total area is obtained by adding the areas of the intervals.

The design of the SCN is based on the thermal model proposed by Martínez-Rodríguez et al. [17] to supply the thermal load at the target temperature, where the number of collectors connected in series provides the target temperature and the number of collectors connected in parallel provides the thermal heat load, as represented in Fig. 2. The design variables of the collector network are geometric dimensions and characteristics of the flat plate collector materials, the properties of the working fluid, the operating conditions of the process and the environmental parameters. The determination of the absorber surface is considered to operate in the most critical conditions of the year, the winter period from Mexico.

The minimum number of collectors in series, N_s, can be determined considering the difference between the outlet temperature T_o^n ($°C$) and inlet temperature T_o^{n-1} ($°C$) to the solar collector is given by Eq. (3):

$$\Delta T = T_o^n - T_o^{n-1} \tag{3}$$

The minimum temperature difference for a solar collector must be 1 °C, that is, $T_o^n - T_o^{n-1} \geq 1$, to be able to include a collector in the series. The number of collector series in parallel, N_p, is calculated by

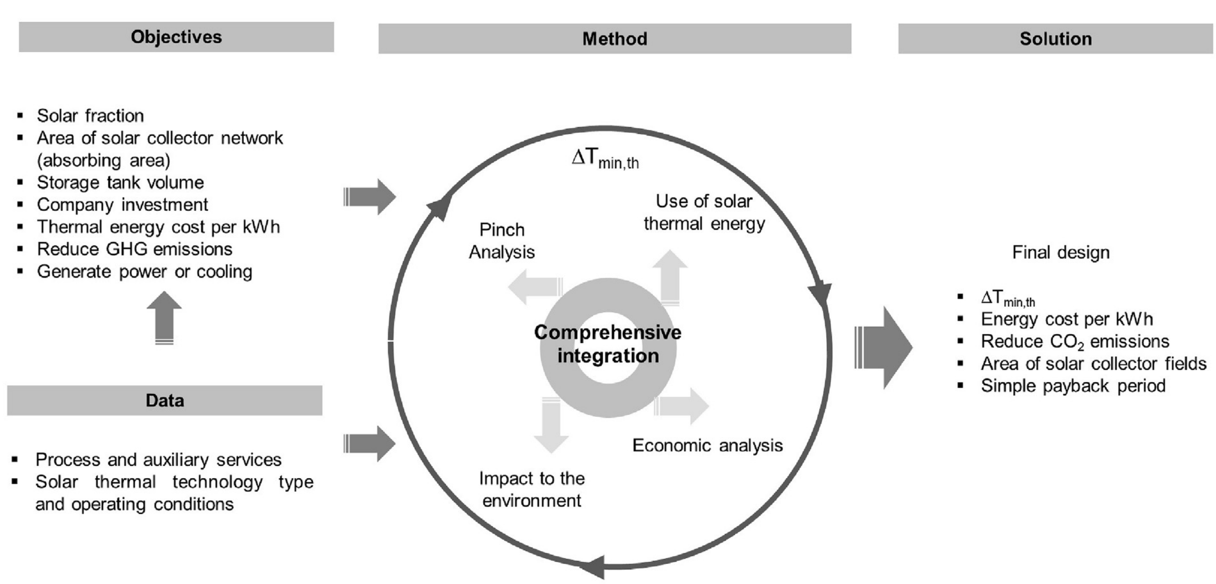

Fig. 1. Design approaches proposed.

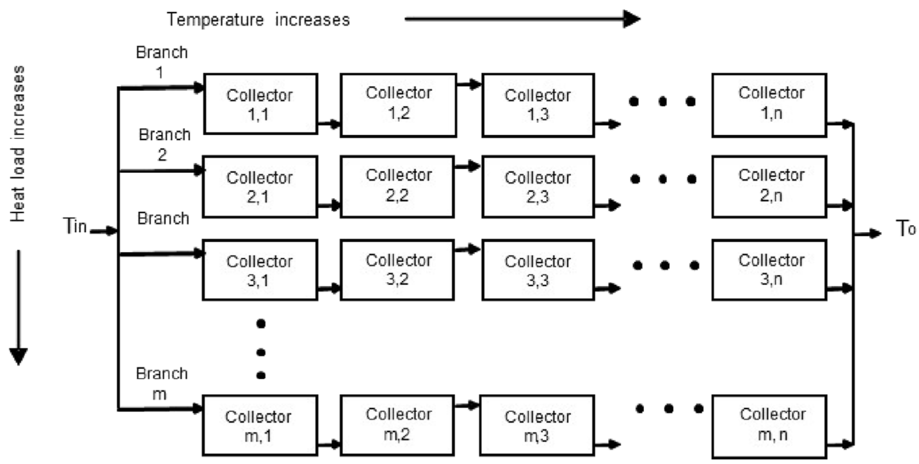

Fig. 2. Representation of a network of solar collectors [adapted from 33].

Eq. (4):

$$N_p = Q/Q_s \tag{4}$$

Where, Q_s (kW) is thermal load that provides a line of n collectors connected in series (Fig. 2) and, Q (kW) is the total thermal load required by the process.

The number of solar collectors, N_c, that make up the structure of the solar field is obtained from Eq. (5):

$$N_c = N_p N_s \tag{5}$$

The surface area of the SCN is calculated using Eq. (6):

$$A_{SCN} = LWN_c \tag{6}$$

where A_{SCN} is the area of SCN (m^2), N_c is the number of solar collectors, L is the length (m) and W (m) is the width of the solar collector.

The calculated areas of heat recovery and SCN present a behavior opposite to each other, by increasing the ΔT_{min}. The area of the heat recovery network (A_{HRN}) decreases with the increase of the minimum temperature difference, ΔT_{min}.

With a fixed ΔT_{min}, the relationship between the calculated areas presents substantial differences. The SCN area is 14 times larger than the area of heat recovery network, Fig. 3, and the cost of heat recovery network is 2.3 times larger than SCN cost. This implies an evaluation of the costs and a negotiation between the costs and the value of the areas, both the area available for installation, as well as the area of the SCN and the heat recovery area.

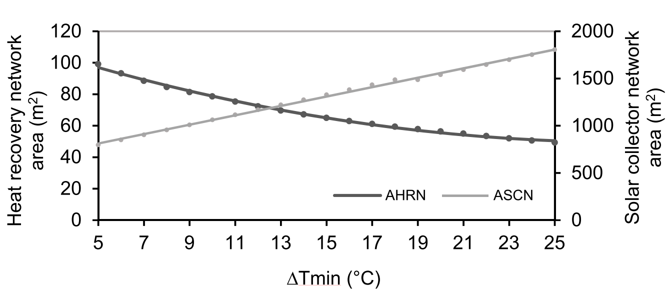

Fig. 3. Comparison of the behaviour of the areas regard to ΔT_{min} for the integration of solar thermal energy. Bold line represents the area of heat recovery network, light line represents the area of solar collector network.

2.2. Costs estimation of system components

In any of the evaluated scenarios to integrate solar thermal technology the costs are involved. Next, the equations with which the costs were evaluated are described (costs from: heat recovery network, auxiliary services, SCN and storage system). The cost of kWh for the solar system and for the integrated system were estimated from the cost of the system (solar or integrated) and the energy produced by the system.

The cost evaluation of the heat recovery network (C_{HRN}) was carried out by Eq. (7) [30],:

$$C_{HRN} = N_e \left[a + b \left(\frac{A_{HRN}}{N_e} \right)^c \right] \tag{7}$$

where is the number of heat exchangers, $a_,$ area of heat recovery network (b), c, 26600 and 6500 are cost constants that are related to construction materials, pressure and type of heat exchanger, the corresponding values are 0.9, C_{US} and [30].

To calculate the cost of utility system, Q_c, Eq. (8) [30], is used. In this equation, the amount of hot utility, that is supplied by the SCN must be considered and subtracted from the total required utility, this to reduce the cost of using said utility.

$$C_{US} = Q_h \cdot C_{USH} + Q_c \cdot C_{USC} \tag{8}$$

where Q_h and Q_c are the heating and cooling requirements of the process, respectively, (kW), C_{USH} and C_{USC} are the costs associated with steam and cooling water, respectively. For the present study, were taken the costs of heating, 150 $USD/(kW\ y)$, and cooling services, 35 $USD/(kW\ y)$ [30].

Then we proceed to determine the cost of the collector network, C_{SCN}, by means of Eq. (9) [31]:

$$C_{SCN} = N_c \left[\gamma_0 + \frac{A_t N_t}{\pi} \left(\gamma_1 d + \gamma_2 + \frac{\gamma_3}{d} \right) + WL\gamma_4 + \gamma_{10} \frac{\dot{m} L \mu}{\pi \rho d^4} \right] + \gamma_5 \left(\frac{\dot{m} H_b}{e_{ff}} \right) \tag{9}$$

where N_c is the number of collectors, A_t is the lateral area of the tube (m^2) [17], N_t is the number of tubes, d is the internal diameter of a tube (m), W and L are the width and length of a solar collector (m), H_b (kW) and e_{ff} are the pump load and efficiency, respectively, and γ_0, γ_1, γ_2, γ_3, γ_4, γ_5, γ_{10} are setting constants.

The cost of the STE storage system, C_{TSS}, is conditioned by the dimensioning of the collector network and the supply time required by the process. Next, Eq. (10) is to determine the cost of thermal storage system [32].

$$C_{TSS} = a' + b' \cdot V_{TSS}{}^{c'} \tag{10}$$

where a', b' and $c'$are cost constants for tanks [33], their values are 5800, 1600 and 0.7, respectively. And V_{TSS} is the volume of the thermal storage system (m^3) determined by Eq. (11) [32]:

$$V_{TSS} = \frac{3600 \cdot Q_{TSS} \cdot t}{CP \cdot \Delta T_{TSS} \cdot \rho \cdot \eta_{TSS}} \tag{11}$$

where Q_{TSS} is the total heat load that is stored at day (kW), t is the total supply time of the process (h), CP ($J/kg\ °C$) and ρ are the heat capacity-mass flow rate of heat transfer fluid and the density or working thermal fluid (kg/m^3), commonly water. ΔT_{TSS} and η_{TSS} are the temperature variation ($°C$) and the efficiency of the thermal storage system, respectively. From this equation the only variable value is the thermal load, therefore there will be a storage volume and a total cost associated with the evaluated ΔT.

Next step is to calculate the total cost ($) of the integrated system, $C_{T\ IS}$. The $C_{T\ IS}$ is the sum of the utility system cost, C_{US}, the cost of the heat recovery network, C_{HRN}, and the cost of the thermal storage system, C_{TSS} Eq. (12), [15]. Since the values of the cost constants in Eqs. (7) and (10) are calculated for the year 2010, to obtain the updated cost values, multiply the costs obtained by the value of the ratio that exists between the cost index for the year 2019 and the cost index for the year 2010, which are 607.5 and 550.8, respectively.

$$C_{T\ IS} = C_{HRN} + C_{SCN} + C_{TSS} + C_{US} \tag{12}$$

In addition, it is necessary to obtain the amount equivalent to a cost per unit of time, in this case an annual cost or annualised cost ($\$/y$) is our interest. The calculation is done with Eq. (13) [30]. Where i is the annual interest and n is the number of years of useful life of a piece of equipment or an equipment network.

$$C_{TA\ IS} = C_{T\ IS} \cdot \left[\frac{i \cdot (1+i)^n}{(1+i)^n - 1}\right] \tag{13}$$

By obtaining the $C_{TA\ IS}$ it is possible to relate each of the variables involved in the integration of energy. That is, not only is the $\Delta T_{min,th}$ determined to obtain the minimum cost of the components of the integrated system, but there is also the possibility of showing the behaviour of different variables depending on the objectives set by the user.

The simple payback time is another criterion of interest in the evaluation of investments. Can be calculated by Eq. (14), both for the solar thermal system and for the integrated system. This criterion relates the total cost of the system in USD and the cost of fossil fuel saved per year.

$$Payback = \frac{total\ systemcost}{S} \tag{14}$$

The costs of heat recovery network C_{HRN}, the SCN, C_{SCNA}, and the STE storage system, C_{TSSA}, were annualised to 25-years using 5% interest. In the same way the energy cost (USD/kWh) was levelised. This approach relates the costs of the energy supply system investment with the energy generated by this system during its useful life (25-years).

CO_2 emissions from natural gas combustion, were quantifying using the factor 0.203 kg/kWh, published by the Ministry of Ecological Transition of the Government of Spain (April 2019) corresponding to fixed combustion equipment.

2.3. Solar fraction

The solar fraction equal to one could be an objective, however, exists restrictions related with space, economical and by temperature levels. Fig. 4 shows the behaviour of STE cost (USD/kWh), with a fixed heat duty and different values of ΔT_{min} and solar fraction. It can be observed, for the same ΔT_{min}, that cost of the kWh_{th} varies significantly with solar fraction, from 0.01 USD/kWh to 0.05 USD/kWh. The cost of the kWh_{th} does not vary with ΔT_{min} when solar fraction is constant.

For the same conditions, the integrated system energy cost (kWh_{is}) varies significantly with solar fraction, while ΔT_{min} increases, Fig. 5. For a fixed solar fraction, the kWh_{is} cost decreases while ΔT_{min} increases.

The comprehensive integration of STE offers a wide range of possibilities; it is possible to have more than one objective on the final solar system. The design approach could be applied to both continuous and batch processes.

Once the $\Delta T_{min,\ th}$ has been defined based on the objective sought, the Grand Composite Curve is used to deliver the hot utility in two temperature levels and increase the supply time of the original SCN. In this scenario it is possible to have an excess of energy and produce another auxiliary service like power or cooling or reduce the size of the SCN. The SCN was designed with the lower irradiance levels on the year to guarantee the heat load demanded by the industrial process during all year.

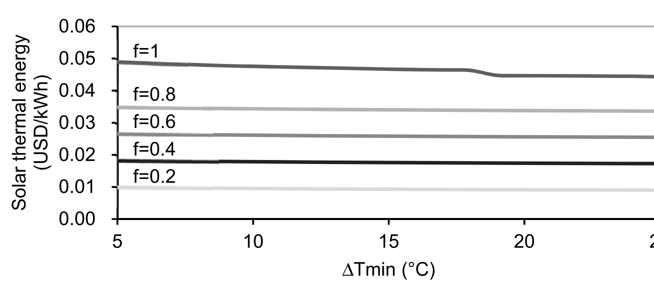

Fig. 4. Behaviour of solar thermal energy cost against different values of ΔT_{min} and solar fraction.

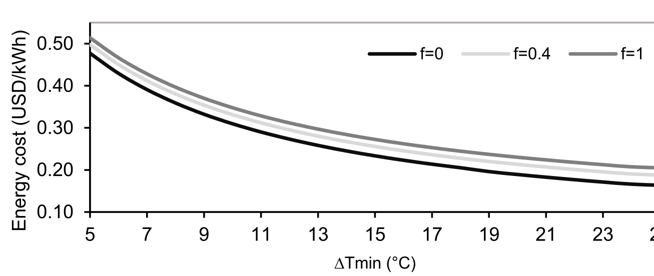

Fig. 5. Behaviour of integrated system cost against different values of ΔT_{min} and solar fraction.

Lastly, the approach will be applied on two study cases. A dairy process and 2G bioethanol process.

3. Case studies

3.1. Dairy industry

Dairy processes encompass a lot of staple food products and by-products. These processes handle operating temperatures below 100 °C, so the process temperature levels are in correspondence with the temperature levels reached by the SCN network, and it could be possible to supply the total thermal load required by the process.

3.1.1. Description of the production process

The case study of a dairy product process described in the literature [34] operates in batches and the heating utility is required in a period of 5 *h*, from 8:00 to 13:00. Fig. 6 shows the diagram of main operations of the dairy production process. The thermal load is 4,401 *kW* and must be supplied to the process for 5 h (8:00 a.m. to 1:00 p.m.).

3.1.2. Detailed solar thermal integration of dairy process

The start point of the integration is define what are the objectives in relation with the process data and the variables considered in method. Table 1 shows the data of the process streams used for Pinch Analysis: where T_{inlet} and T_{outlet} are the inlet and outlet temperatures of the streams (°C), respectively, and CP is the heat capacity of the current ($kW/°C$). With the data of the streams the minimum hot utilities are calculated. Values of heat transfer coefficients considered in this case are 0.8 $kW/(m^2\ °C)$ for water and slightly viscous substances and 0.3 $kW/(m^2\ °C)$ for viscous substances.

Designing the collector network for dairy industry case study, a target temperature of 100 °C is set and the thermal load levels vary according to the evaluated ΔT_{min}. For example, for a $\Delta T_{min} = 5$ °C the solar collector area, with 435 units, is 796 m^2. These values increase as the ΔT_{min} does the same one; in the same way rising of the requirement of thermal load (minimum hot utilities).

Once the energy requirements of the process have been determined using Pinch Analysis, the different costs associated with the heat recovery network and utilities are calculated. In addition, it is possible to determine the solar fraction that can be achieved by integrating STE, through a network of solar collectors. With this, it seeks to increase the supply time, by determining temperature levels below the maximum. Figs. 7 and 8 show the location of Pinch point and thermal loads corresponding to each temperature level by varying ΔT_{min}. GCC is constructed with modified temperatures, whereby the heating service supply, in Fig. 7 is at 99 °C for $\Delta T_{min} = 8$ °C, and in Fig. 8 is at 104 for a °C = 18 ΔT_{min}. Comparing the information provided by both curves, it is seen the supply temperature for Fig. 7 is 95 °C with a heat load of 265 °C, while for Fig. 8 the supply kWtemperature is also 95 °C, however, the thermal load is increased to 415 kW. In both cases the temperature level

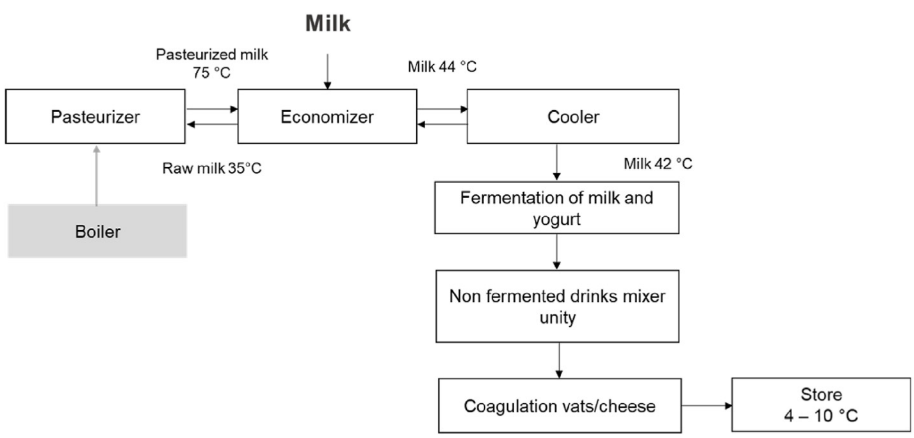

Fig. 6. Diagram of the main stages of the dairy product process.

Table 1
Dairy process stream data.

Streams	Description	T_{inlet} (°C)	T_{outlet} (°C)	CP (kW/°C)
H1	Effluent pasteurised milk	75.00	44.00	4.38
H2	Boiler water	95.00	78.00	10.63
H3	Input milk	44.00	36.00	5.84
H4	Water of the storage tank	73.30	40.00	1.94
H5	Water of the rennet vats	40.00	38.00	3.89
H6	Water of the storage tank	62.40	25.00	9.30
H7	Water of the storage tank surplus	62.40	25.00	12.90
C1	Mains water for boiler	12.20	95.00	10.63
C2	Raw milk input	4.00	35.00	4.38
C3	Milk input	35.00	75.00	4.38
C4	Mains water for cooler	12.20	18.00	6.35
C5	Mains water	12.20	38.00	2.64
C6	Milk from rennet vats	34.00	35.00	3.89

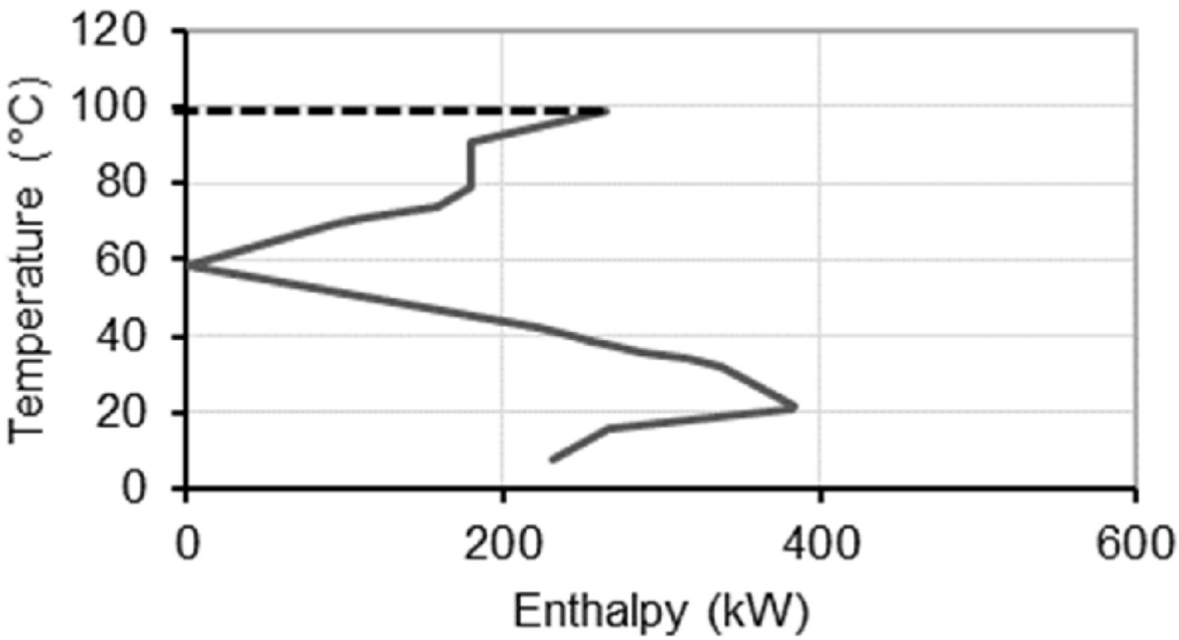

Fig. 7. Grand Composite Curve, $\Delta T_{min} = 8°C$, dairy process.

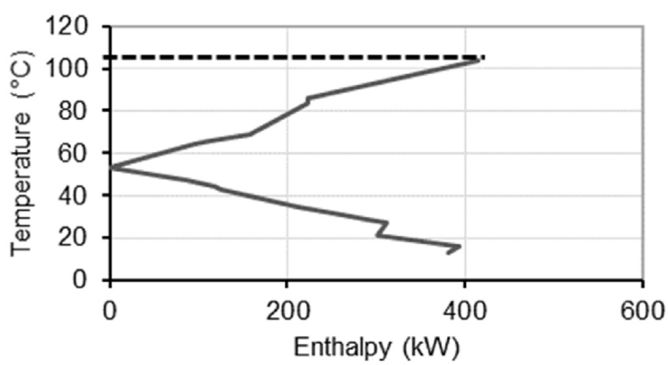

Fig. 8. Grand Composite Curve, $\Delta T_{min} = 18$ °C, dairy process.

for the energy requirement can be supplied with low-temperature solar collectors, and the solar fraction is 1.

Continuing with the procedure outlined in section 2.1, Table 2 shows the results of the utilities (Q_h and Q_c), the area of heat recovery network (A_{HRN}) and the costs for the dairy industry by varying ΔT_{min} from 5 °C to 25 °C. The Pinch temperatures are below of the SCN target temperature. The minimum hot utility increases 58%, changing from 220 kW to 522 kW while the area of heat recovery network reduces 60%.

For all the ΔT_{min} considered in dairy process, 5 to 25 °C, the solar fraction is one. It means that it is possible to deliver total heat duty with STE. The selected scenario will depend on the STE integration available total area, the costs of solar system and integrated system. Table 3 shows the relationship between the $\Delta T_{min,th}$, area of solar

Table 2
Costs of the heat recovery network, utility systems and cost of energy integration for different ΔT_{min}, in a dairy process.

ΔT_{min} (°C)	Q_h (kW)	Q_c (kW)	$T_{pinchshifted}$ (°C)	A_{HRN} (m^2)	C_{HRN} ($)	C_{HRNA} ($\$/y$)	C_{US} ($\$/y$)	C_{TA} ($\$/y$)
5	220	186	59.9	324	2,228,359	158,108	39,457	197,564
6	235	201	59.4	298	2,105,172	149,367	42,234	191,601
7	250	216	58.9	277	2,003,373	142,144	45,010	187,155
8	265	231	58.4	260	1,917,042	136,019	47,787	183,806
9	280	246	57.9	245	1,842,409	130,723	50,564	181,288
10	295	261	57.4	231	1,776,863	126,073	53,341	179,414
11	310	276	56.9	220	1,718,732	121,948	56,118	178,066
12	325	291	56.4	209	1,666,687	118,256	58,895	177,150
13	340	306	55.9	200	1,619,710	114,922	61,672	176,594
14	355	321	55.4	192	1,577,005	111,892	64,448	176,341
15	370	336	54.9	184	1,537,932	109,120	67,225	176,345
16	385	351	54.4	177	1,501,988	106,570	70,002	176,572
17	400	366	53.9	170	1,468,775	104,213	72,779	176,992
18	415	381	53.4	164	1,437,955	102,026	75,556	177,582
19	430	396	52.9	159	1,409,268	99,991	78,333	178,324
20	445	411	52.4	154	1,382,478	98,090	81,110	179,200
21	460	426	51.9	149	1,357,385	96,310	83,886	180,196
22	475	441	51.4	144	1,331,230	94,454	86,663	181,117
23	490	456	50.9	139	1,306,563	92,704	89,440	182,144
24	505	471	50.4	135	1,283,245	91,049	92,217	183,266
25	522	487	49.9	130	1,293,338	91,766	95,287	187,052

Table 3
Relationship between ΔT_{min} with size of the solar collector network and the thermal storage system.

ΔT_{min} (°C)	Q_h (kW)	Solar fraction (f)	SCN array	Area of SCN (m^2)	C_{SCN} ($\$$)	V_{TSS} (m^3)	C_{TSS} ($\$$)	Solar thermal payback (y)
5	220	1.00	15x29	796	244,195	21	21,299	1.9
6	235	1.00	16x29	849	259,632	23	22,004	1.9
7	250	1.00	17x29	902	275,058	24	22,696	1.9
8	265	1.00	18x29	955	290,474	25	23,376	1.9
9	280	1.00	19x29	1008	305,289	27	24,044	1.9
10	295	1.00	20x29	1061	321,275	28	24,702	1.9
11	310	1.00	21x29	1114	336,662	30	25,349	1.9
12	325	1.00	22x29	1168	352,041	31	25,988	1.9
13	340	1.00	23x29	1221	367,413	33	26,617	1.8
14	355	1.00	24x29	1274	382,777	34	27,238	1.8
15	370	1.00	25x29	1327	398,135	35	27,851	1.8
16	385	1.00	26x29	1380	413,486	37	28,457	1.8
17	400	1.00	27x29	1433	428,831	38	29,056	1.8
18	415	1.00	28x29	1486	444,170	40	29,648	1.8
19	430	1.00	28x29	1486	444,170	41	30,234	1.8
20	445	1.00	29x29	1539	459,503	43	30,814	1.8
21	460	1.00	30x29	1592	474,832	44	31,387	1.8
22	475	1.00	31x29	1645	490,155	46	31,956	1.8
23	490	1.00	32x29	1698	505,473	47	32,518	1.7
24	505	1.00	33x29	1751	520,786	48	33,076	1.7
25	522	1.00	34x29	1804	536,095	50	33,687	1.7

system (includes the area of SCN and solar energy storage system) and the associated costs. The simple payback time practically is constant.

The annualised costs of each component of the integrated solar thermal system change significantly with the increase of ΔT_{min}. The cost of auxiliary services and annualised cost of the solar energy storage system are notably lower with respect to the annualised costs of SCN and heat recovery network. These relations can be used to achieve different design objectives of the solar thermal system.

Fig. 9 shows the trend of annualised costs of heat recovery network (C_{HRNA}) and the integrated solar thermal system ($C_{TA\ IS}$). Both curves present a similar behaviour with a minimum point as it increases ΔT_{min}. However, the selection of the objective will define $\Delta T_{min,\ th}$. The difference between both curves is given by the non-linear increase in hot minimum utility.$C_{TA\ IS}$

Greenhouse gas emissions are zero in all cases, because it is possible to eliminate the use of fossil fuels. Although this objective is covered with each CO_2, another additional objective is sought. Table 4 shows the results obtained when evaluating the kWh, emissions, the costs of the energy, in kWh_{th} for the solar system (kWh_{is}) and of the integrated solar thermal system (), for the different ΔT_{min}. Making a comparison between the cost of kWh_{th} and the cost of kWh_{is}, the latter is larger by approximately 3.6–9.7 times, and its absolute value decreases very significantly with the increase of ΔT_{min}.

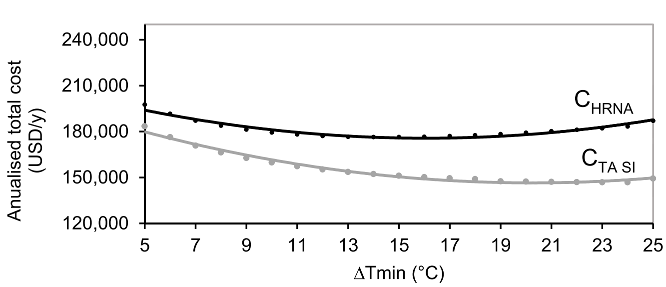

Fig. 9. Behaviour of annualised cost of the integrated solar thermal system, $C_{HRNA,}$ and the annualised cost of the heat recovery network, $\Delta T_{min,}$ at different ΔT_{min}.

Table 4
Determination of CO_2 emissions and energy cost for different ΔT_{min}.

ΔT_{min} (°C)	CO_2emissions (ton/y)	kWh_{th}($\$/kWh$)	kWh_{is}($\$/kWh$)
5	0	0.0490	0.4771
6	0	0.0486	0.4293
7	0	0.0483	0.3908
8	0	0.0481	0.3591
9	0	0.0477	0.3323
10	0	0.0476	0.3097
11	0	0.0474	0.2901
12	0	0.0472	0.2731
13	0	0.0470	0.2583
14	0	0.0469	0.2451
15	0	0.0467	0.2335
16	0	0.0466	0.2230
17	0	0.0464	0.2137
18	0	0.0463	0.2052
19	0	0.0447	0.1961
20	0	0.0447	0.1891
21	0	0.0446	0.1828
22	0	0.0446	0.1768
23	0	0.0445	0.1713
24	0	0.0445	0.1662
25	0	0.0443	0.1635

3.2. 2G bioethanol industry from agave

Second generation of bioethanol production process uses agave as its raw material. This case study is of significant relevance, since Mexico is one of the countries with the largest areas of cultivation of this plant worldwide. The revised industrial process is based on the work of Oseguera-Villaseñor [35].

3.2.1. Process description

The process for obtaining bioethanol from agave is graphically described in Fig. 10. Tequila and mezcal industry, only takes advantage of 40% by weight of this product when processing the pineapple from agave. After performing a mechanical separation, the pineapples go to a cooking process, completing this task, a part enters together with the agave bagasse to a grinding process where acid hydrolysis is carried out, a fraction of the output enters an enzymatic hydrolysis as waste, the output of both processes is fed to the fermentation process; lignin is obtained from enzymatic

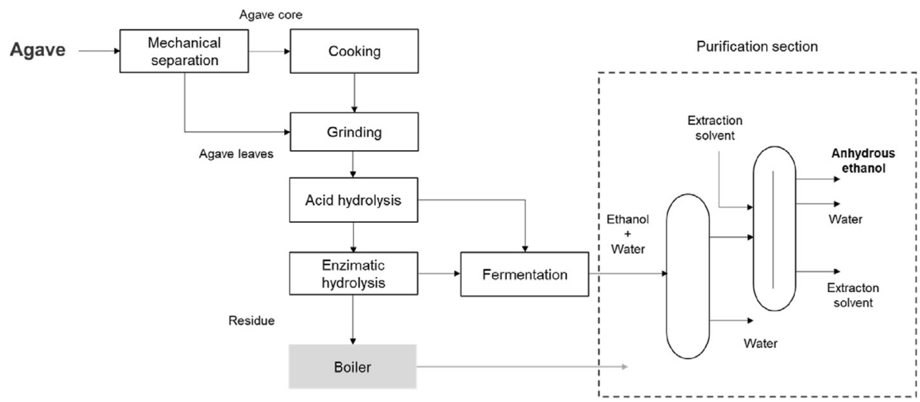

Fig. 10. Block diagram of the bioethanol production process from agave.

hydrolysis, which can be used as a biofuel.

After fermentation, the ethanol-water mixture enters an ethanol purification process, whatever the raw material or the process, the product obtained from the fermentation is a dilute solution of less than 10% by weight of ethanol. In the bioethanol purification process a conventional distillation column is used, there, the mixture must be brought as close to the azeotrope as possible, the distillate then passes to a second column where a second purification is carried out using a mass extraction solvent, the purity specified is 99.5% so that it can be used as an additive mixed with gasoline.

The bioethanol purification operation demands the highest energy consumption in the process. The thermal load required for purification is 97,915 kWh in a process that operates 24 h for 350 days a year. A natural gas boiler generating 205 °C of saturated steam provides this service.

3.2.2. Detailed solar thermal integration for bioethanol process

In this work, the integration of STE will be carried out in the ethanol purification section. Table 5 shows the data of the process streams that will be used for the integration of STE.

The values of the convective heat transfer coefficients considered in this case are 0.8 $kW/(m^2\ ^\circ C)$ for water and slightly viscous substances and 0.3 $kW/(m^2\ ^\circ C)$ for viscous substances.

Using Pinch Analysis, the energy requirements of the process and the amount of energy that can be supplied with the integration of STE, using a network of low-temperature solar collectors are determined. Table 6 shows the energy and cost results of heat recovery network, evaluated between 5 and 25 °C. The Pinch temperature is far below of the target temperature (105 °C) delivered for the SCN. By varying the ΔT_{min} from 5 °C to 25 °C, the minimum hot utility increases 59%, which impacts on the annualised total cost.

As stated in the method, once the energy requirements of the process have been obtained, the design of the SCN is carried out, the supply temperature to the process is 105 °C and the environmental parameters considered were from winter period. The design of the network is carried out considering a supply time of 24 h. Table 7 shows the solar fraction, f, which indicates the amount of heat that the process will receive from a SCN, $Q_{h\ SCN}$. Next, the costs of the network and the design, and costs of the thermal storage system are obtained, the latter is related to the heat supply time and the temperature level required by the process. Temperature levels from the minimum hot utility after $\Delta T_{min} = 5\ ^\circ C$, could not be reached by a low-temperature SCN. The simple payback time almost is constant. In this study case the CO_2 emissions could be until 391 ton/y. The area of SCN required for supply the heat load is significantly bigger, compared with the absorber area for dairy process.

Once the minimum utilities, hot and cold, have been defined, starting from ΔT_{min}, the following analysis focuses on locating the levels of utilities and matching them with the solar thermal availability, based on the selected collector network, maximising the use of STE and reducing the costs of services. Unlike the dairy case study, where in all ΔT_{min} the solar fraction is equal to one, in the bioethanol process this only occurs with a $\Delta T_{min} = 5\ ^\circ C$.

Table 5
Data of the 2G bioethanol production process streams.

Streams	Description	T_{inlet} (°C)	T_{outlet} (°C)	CP (kW /°C)
H1	Ethanol-water	78.23	78.20	11,888.33
H2	Water SA-R1	185.22	100.00	3.27
H3	Anhydrous ethanol	78.57	78.28	434.44
H4	Water SA-R2	204.00	185.22	4.27
H5	Side stream water	106.00	20.00	1.19
H6	Glycerol outlet stream	194.00	20.00	6.36
H7	Water outlet stream	100.00	20.00	38.82
C1	Ethanol-water	20.00	79.00	59.83
C2	Water SA-C1	20.00	62.87	8.31
C3	Ethanol-water R1	99.97	100.00	9,308.00
C4	Water SA-C2	20.00	35.68	8.03
C5	Ethanol-glycerol R2	107.68	194.88	0.92
C6	Glycerol	20.00	194.00	6.84

4. Analysis of results

Based on results obtained for an industrial process, exist many objectives that could be reached when carrying out a comprehensive integration of STE. The set of objectives and variables are analysed to have a panoramic view of the process needed in making decisions. Checking the results, it is possible to identify scenarios where the solar fraction is equal to one, maximising the heat exchanger process to process, and minimising the hot utility and the size of SCN. Cost is the variable that define the viability of the solar system, and with that, the integration of the STE.

4.1. Dairy process scenarios

4.1.1. Scenario 1

Objectives: minimum cost of the heat recovery network, solar fraction equal to one and increasing the operation time of the SCN.

The minimum cost of heat recovery network is the variable most significant in the integration of STE in the process. For this case, the $\Delta T_{min,th}$ is 14 °C, the thermal load is 355 kW and it can be supplied

Table 6
Results of the energy integration of bioethanol production process from agave to different ΔT_{min}.

ΔT_{min} ($^\circ C$)	Q_h (kW)	Q_c (kW)	$T_{pinch\ shifted}$ ($^\circ C$)	A_{HRN} (m^2)	C_{HRN} ($)	C_{HRNA} ($/y)	C_{US} ($/y)	C_{TA} ($/y)
5	637	232	22.5	854	4,155,997	336,158	103,635	439,793
6	683	278	23.0	808	3,973,698	321,413	112,216	433,629
7	730	325	23.5	763	3,795,348	306,987	120,797	427,784
8	776	371	24.0	722	3,630,084	293,619	129,378	422,997
9	822	417	24.5	689	3,497,874	282,926	137,959	420,884
10	869	464	25.0	660	3,381,395	273,504	146,540	420,044
11	915	510	25.5	634	3,277,754	265,121	155,120	420,241
12	961	557	26.0	611	3,184,790	257,602	163,701	421,303
13	1,008	603	26.5	594	3,116,174	252,052	172,282	424,334
14	1,054	649	27.0	575	3,039,793	245,874	180,864	426,737
15	1,101	696	27.5	559	2,970,570	240,275	189,444	429,719
16	1,147	742	28.0	547	2,922,980	236,425	198,024	434,450
17	1,193	789	28.5	533	2,866,763	231,878	206,605	438,483
18	1,240	835	29.0	521	2,815,016	227,693	215,187	442,879
19	1,286	881	29.5	509	2,767,253	223,829	223,767	447,596
20	1,333	928	30.0	499	2,723,087	220,257	232,348	452,604
21	1,379	974	30.5	489	2,682,155	216,946	240,929	457,876
22	1,425	1,020	31.0	480	2,644,155	213,872	249,510	463,382
23	1,472	1,067	31.5	471	2,608,823	211,015	258,090	469,105
24	1,518	1,113	32.0	463	2,575,918	208,353	266,671	475,024
25	1,564	1,160	32.5	456	2,545,238	205,872	275,252	481,124

Table 7
Results of the integration of solar thermal energy from the bioethanol production process from agave to different ΔT_{min}.

ΔT_{min} ($^\circ C$)	Q_{hSCN} (kW)	f	A_{SCN} (m^2)	C_{SCN} ($)	C_{SCNA} ($/y)	V_{TSS} (m^3)	C_{TSS} ($)	C_{TSSA} ($/y)	CO_2 emissions (ton/y)	Solar thermal Payback (y)	kWh_{th} ($/kWh)	kWh_{is} ($/kWh)
5	637	1.00	9,393	2,706,553	192,037	260	288,027	20,436	0	1.76	0.0897	0.1061
6	584	0.86	10,030	2,887,894	204,903	278	301,042	21,360	169	1.75	0.1031	0.0992
7	624	0.86	10,720	3,084,272	218,837	296	313,803	22,265	181	1.75	0.1017	0.0934
8	663	0.86	11,357	3,265,479	231,694	314	326,331	23,154	192	1.74	0.1002	0.0883
9	703	0.86	11,994	3,446,629	244,547	333	338,643	24,028	204	1.74	0.0988	0.0841
10	742	0.86	12,684	3,642,815	258,467	351	350,754	24,887	216	1.74	0.0977	0.0807
11	782	0.85	13,321	3,823,858	271,312	369	362,679	25,733	227	1.73	0.0965	0.0777
12	821	0.85	14,010	4,019,936	285,224	387	374,428	26,567	239	1.73	0.0956	0.0751
13	861	0.85	14,647	4,200,885	298,063	405	386,013	27,389	251	1.73	0.0946	0.0730
14	900	0.85	15,284	4,381,793	310,899	424	397,442	28,199	262	1.72	0.0936	0.0709
15	940	0.85	15,974	4,577,733	324,801	442	408,725	29,000	274	1.72	0.0929	0.0692
16	980	0.85	16,611	4,758,562	337,632	460	419,870	29,791	286	1.72	0.0921	0.0677
17	1019	0.85	17,248	4,939,357	350,459	478	430,883	30,572	297	1.71	0.0913	0.0662
18	1060	0.86	18,097	5,180,365	367,560	501	444,232	31,519	306	1.72	0.0912	0.0652
19	1098	0.85	18,575	5,315,907	377,177	515	452,540	32,109	321	1.71	0.0899	0.0638
20	1138	0.85	19,211	5,496,604	389,998	533	463,195	32,865	332	1.71	0.0893	0.0627
21	1177	0.85	19,901	5,692,326	403,885	551	473,742	33,613	344	1.71	0.0887	0.0618
22	1217	0.85	19,530	5,586,941	396,407	542	468,343	33,230	356	1.71	0.0846	0.0598
23	1256	0.85	19,211	5,496,604	389,998	532	462,916	32,845	367	1.71	0.0808	0.0581
24	1296	0.85	18,893	5,406,259	383,587	523	457,461	32,458	379	1.71	0.0773	0.0565
25	1335	0.85	18,521	5,300,848	376,108	514	451,975	32,069	391	1.71	0.0738	0.0549

at 100 $^\circ C$ with a network of 696 flat-plate solar collectors and a thermal storage volume of 34 m^3 (see Table 3, Section 3.1.2). To supply the thermal load required by the process, the SCN operates for 3 h (11:15 a.m. to 2:15 p.m.). Designing of the SCN, however, was developed considering that STE will not be fed to the process directly from the network. But rather that, the entire thermal load required by the process will be stored to be supplied the next day during 5 h of operation (8:00 a.m. to 1:00 p.m.). By matching the temperature of multiple utility targets with the solar availability at the different temperature levels required by the process, at the selected $\Delta T_{min,th}$, the thermal energy requirement can be supplied at two temperature levels, that is, 157 kW at 71 $^\circ C$ and 198 kW at 100 $^\circ C$, as shown in Fig. 11.

In this case, it is possible to design 2 smaller SCN that meet the heat loads, as result the absorber area decreases by 24%, this is due part of the thermal load is provided at lower level of temperature, increasing the period of operation of the solar field, and consequently decreases the number of parallels of the network. The results of these assertions can be seen in Table 8.

4.1.2. Scenario 2

The same objectives are sought as in the previous scenario and additional way to generate power.

If using the original SCN, that is, a network with 696 solar collectors, there would be a 21% surplus of hot water at 100 $^\circ C$. This would be achieved by identifying two levels of temperature (71 $^\circ C$ and 100 $^\circ C$) to supply the heat duty to the process. It means the original design of the SCN is oversized; an excess of thermal energy is generated. This surplus could be used to generate another service, for example electricity. All this in addition to complying with the reduction of CO_2 emissions and lower cost of the heat recovery network.

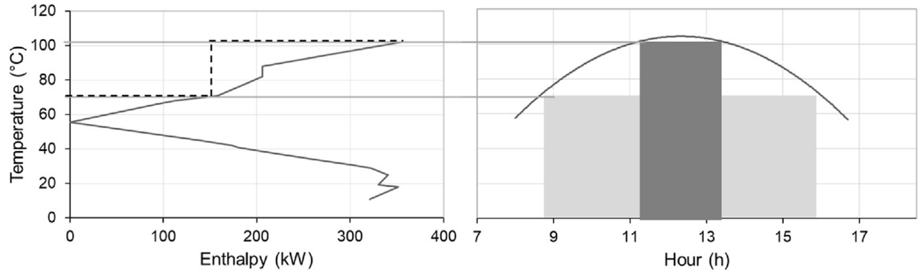

Fig. 11. Pairing temperatures of multiple utility targets with the availability of solar energy for the dairy process ($\Delta T_{min} = 14\,^{\circ}C$).

Table 8
Design of solar collector networks for different thermal loads and required temperature level.

Thermal load (kW)	Supply temperature ($^{\circ}C$)	Operation period (h)	SCN array	Area of SCN (m^2)
355	100	3.00	24x29	1,274
157	71	7.75	4x29	225
198	100	3.00	13x29	732

4.1.3. Scenario 3

Objectives: Solar fraction equal to one, competitive cost of energy in kWh and the smaller absorber area of SCN.

There are some options that can accomplish the objectives. However, the point that defines the selection is the smaller area. The objectives mentioned are met for a $\Delta T_{min,th} = 20\ ^{\circ}C$. At this point, the variation in the cost of energy begins to decrease considerably, it is observed in Fig. 12, after this point the cost of energy in kWh trends to be constant.

Under these conditions, the absorber area of the solar field is 1539 and the STE cost in m^2 is 0.0447 kWh_{th}. Comparing the STE cost, in $USDkWh_{th}$,kWh\$ with the conventional energy system, in $MMBTU$, the ratio is 0.85 times. Currently, the cost of steam produced from conventional sources ranges from $USD/\ kWh$ 12–15 per (ie 0.0410–0.0520 kWh).

4.2. 2G bioethanol process scenarios

4.2.1. Scenario 1

Objectives: minimum cost of the heat recovery network, solar fraction equal to one and increase the operation time of the SCN.

There is only one case where the solar fraction is equal to one. This happens when $= 5\,^{\circ}C$. The STE cost is 0.0897 $USD/\ kWh$ and the absorber area of the solar field is 9,393 m^2. One way to increase or maximise the operation of the solar device is using different temperature levels to supply the heat load required by the process. Fig. 13 is a graph showing the match between multiple utility targets and solar thermal availability of the collector network. For $\Delta T_{min} = 5\,^{\circ}C$ ($\Delta T_{min,\ th}$), the temperature levels of the utilities are 40 $^{\circ}C$ and 103 $^{\circ}C$. The deliver times for each temperature level are 8 h and 2.5 h, with a total thermal requirement of 637 kW. In this scenario, it is possible to supply the entire thermal load of the process with solar energy with a network of 5,133 solar collectors (9,393 m^2). Two levels of temperature are represented and their thermal load, respectively, the thermal requirement is 565 kWat 40 $^{\circ}C$ and 72 kWat 103 $^{\circ}C$.

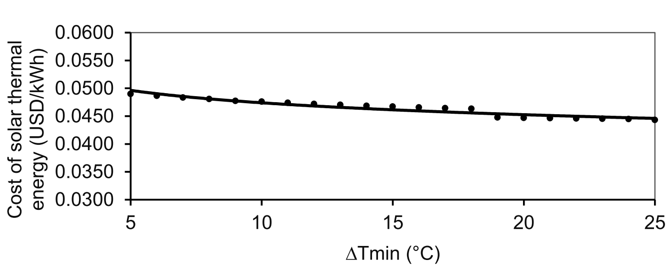

Fig. 12. Cost per kWh_{th} of solar thermal energy (ΔT_{min}) for different $\Delta T_{min,\ th}$.

It is possible to design 2 solar fields that supply the heat load. Keeping the 9,393 m^2 solar field running at two temperature levels will result in an energy surplus of 44%, as the original design reaches 105 $^{\circ}C$. Or, if two solar fields are used that supply thermal loads at 40 $^{\circ}C$ and 105 $^{\circ}C$, the size of the SCN could be reduced by up to 49% as can be seen in Table 9.

4.2.2. Scenario 2

Objectives: Restrictions of available area, reduce CO_2 emissions and energy cost in kWh_{is}.

Restrictions on the absorber area is something that could happen when the solar collector area is big. In this case, the objectives could be accomplished with $\Delta T_{min,\ th} = 6\,^{\circ}C$ with a cost per kWh of solar thermal integrated system of 0.0992 USD. The solar collector area is of 10,030 m^2, emissions of CO_2 to environment are 169 ton/y with a solar fraction of 0.85. In this scenario 99 kW are required at temperature level higher to 105 $^{\circ}C$ of the hot utility.

4.2.3. Scenario 3

Objectives: Lower cost of energy in kWh_{th} and in kWh_{is}, a small SCN and, reduce the emissions of CO_2.

Behaviour of kWh_{th}energy cost is opposite regard to kWh_{is}, when ΔT_{min} increases. In this study case, the solar fraction is almost constant except for $\Delta T_{min} = 5°C$. Thus, the lower cost of energy, without surface limitations to the installation of a solar collector field is reached with a $\Delta T_{min,th}$ of 25 $^{\circ}C$. In this case the absorber area is 18,521 m^2 and the cost of STE in kWh_{th} is 0.0738 USD/kWh. The emissions of CO_2, under this criterion, are 391 ton/y and the cost of integrated energy system, in kWh_{is}, is 0.0549 USD/kWh. However, if there is a limitation for the area of installation of the solar field, it is still possible to accomplish the other two objectives (lower energy cost and emission reduction) with a $\Delta T_{min,th} = 15\,^{\circ}C$. At this point the absorbing area decreases by 14% (final installation area: 15,974 m^2). Now the cost of energy in kWh_{th} and in kWh_{is} are 0.0929 y 0.0692 USD/kWh respectively. The solar fraction is 0.85 and the emissions of CO_2 are 274 ton/y. Fig. 14 shows the trends of

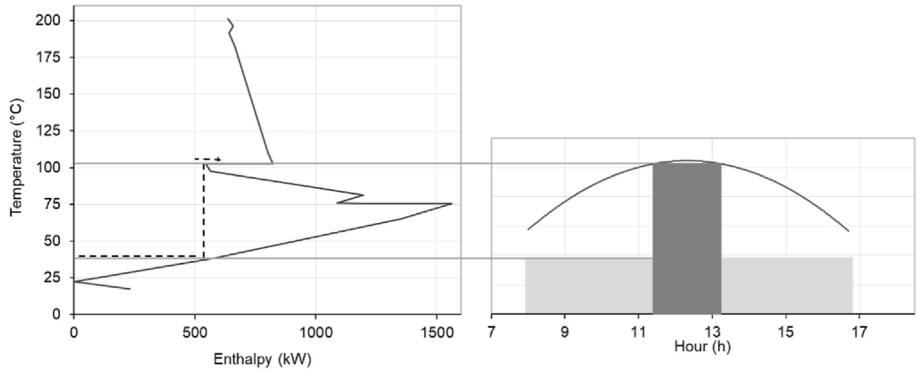

Fig. 13. Pairing temperatures of multiple utility targets with the availability of solar energy for the bioethanol process ($\Delta T_{min} = 5\ ^{\circ}C$).

Table 9
Design of solar collector networks for different thermal loads and required temperature level.

Thermal load (kW)	Supply temperature ($^{\circ}C$)	Operation period (h)	SCN array	Area of SCN (m^2)
637	105	2.5	177x29	9,393
565	40	8.0	67x29	3,556
72	105	2.5	24x29	1,274

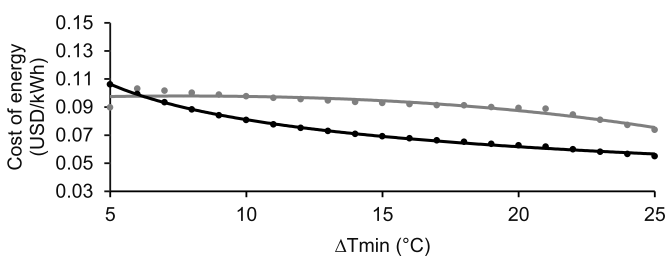

Fig. 14. *Cost per kWh of solar thermal energy for different ΔT_{min}. Trends of kWh_{th} (gray line) and kWh_{is} (black line).*

energy cost. The kWh_{th} (gray line) is more expensive than the kWh_{is} (black line).

5. Conclusions

The proposed design method, comprehensive solar thermal integration for industrial process, let to accomplish multiple objectives, maximising in each one of the scenarios the use of STE, the operation time of the SCN, the solar fraction. In both study cases the Pinch temperature is below 100 $^{\circ}C$.

In each case study, different scenarios were evaluated, and the defined objectives were different depending on the needs of the processes. However, with an approach based on design objectives, it seeks to maximise the integration of STE to have more sustainable processes. With the use of $\Delta T_{min,\ th}$ a design space is opened for the achievement of objectives, which are sought to be attained simultaneously, such as: zero CO_2 emissions, increase in the supply time of the network of solar collectors, production of surplus energy to be used in other forms of energy, adaptation to limited installation surfaces, among others.

In the dairy process case, it was possible to achieve zero CO_2 emissions with low temperature solar thermal collector networks by carrying out a detailed integration that maximises the solar fraction to one, through the analysis of the variables considered in the method. The STE cost, in $kWh_{th,}$ is competitive in all considered cases from 5 $^{\circ}C$ to 25 $^{\circ}C$ with values from 0.0490 to 0.0443 USD/kWh. The cost to produce hot water or vapour using natural gas is 0.0520 USD/kWh.

2G Bioethanol process obtained from agave presented only one result with solar fraction equal to one and $\Delta T_{min} = 5^{\circ}C$. Solar fraction in other cases was constant (0.85). In these cases, the absorber area reached values of 18,521 m^2 and emissions of 6957 ton/y. The STE cost in kWh_{th} reduced up to values of 0.0738 USD/kWh, the ratio with the cost obtained using natural gas was 1.4.

Comparing with other relevant works [10,36], this study opens the possibility of achieving zero CO_2 emissions, in addition to foresee multiple utilities. With the present solar integration approach, the operation of the SCN was determined and it was possible to reduce its area by up to 49% for the bioethanol industry and up to 24% for the dairy industry, or to have energy surpluses of up to 44% for the bioethanol industry and 21% for the dairy industry, in addition to significantly increasing of supply time of the SCN, keeping constant its area and the storage capacity.

The scope of the present design approach is even greater since it could be scaled, for example, with medium temperature solar thermal technology or other design objectives.

Credit author statement

Guillermo Martínez-Rodríguez: Conceptualization, Methodology, Investigation, Writing original draft preparation, Reviewing and editing, Supervision, Project. administration, Visualization. Amanda L. Fuentes-Silva: Software, Data curation, Writing original draft preparation, Formal analysis, Investigation, Artwork. Martín Picón-Núñez: Investigation.

Declaration of competing interest

The authors declare that they have no known competing financial interests or personal relationships that could have appeared to influence the work reported in this paper.

Acknowledgements

The authors warmly appreciate the research experience shared by Ph. D. Juan-Carlos Baltazar from Texas A & M University, as well as the help of Ms. Evangelina Sánchez-García in searching the literature for review and edition of the manuscript.

This research was supported by the National Council for Science and Technology (CONACYT) project 316058, year 2021. The publication of this work was supported by CONACYT, University of Guanajuato and by the Trade Union Association of Administrative Academic Staff (ASPAAUG).

Nomenclature

A	Heat transfer area, m^2
A_k	k Interval area, m^2
A_{HRN}	Heat recovery network area, m^2
A_{SCN}	Solar collector network area, m^2
A_t	Lateral area of raiser tube, m^2
CC	Composite Curve
CP	Heat capacity-mass flow rate of heat transfer fluid, J/kg °C
C_{SCN}	Solar collector network cost, USD
C_{SCNA}	Anualised solar collector network cost, USD/y
C_{HRN}	Heat recovery network cost, USD
C_{HRNA}	Anualised heat recovery network cost, USD/y
C_{US}	Utility system cost, USD/y
C_{USH}	Cost associated with heating service (steam), USD/kW
C_{USC}	Cost associated with cooling water service, USD/kW
C_{TSS}	Thermal storage system cost, USD
C_{TSSA}	Anualised thermal storage system cost, USD/y
$C_{T\ IS}$	Total cost of the integrated solar thermal system, USD
$C_{TA\ IS}$	Anualised total cost of the integrated solar thermal system, USD/y
d	Inner diameter of raiser tube, m
e_{ff}	Efficiency of the pump, dimensionless
GCC	Grand Composite Curve
H_b	Pump load, kW
H	Convective coefficient of a stream, kW / m^2 °C
h_i	Individual convective coefficient of hot stream i, kW/m^2°C
h_j	Individual convective coefficient of cold stream j, kW/m^2°C
i	Annual interest
kWh_{th}	Solar thermal energy, kWh
kWh_{is}	Thermal energy of system integrated, kWh
L	Length of raiser tube, m
LCOEth	Levelised cost of thermal energy
n	Number of years of useful life of an equipment, a network of equipment or a plant, y
N_c	Number of solar collectors of the solar field, dimensionless
N_e	Number of heat exchangers, dimensionless
N_p	Number of series in parallel, dimensionless
N_s	Number of collectors in series, dimensionless
N_t	Number of tubes of solar collector, dimensionless
Q	Total thermal load required by the process, kW
Q_c	Process cooling requirement, kW
Q_{TSS}	Total heat load to be stored in the day, kW
Q_h	Process heating requirement, kW
$Q_{h\ SCN}$	Thermal load supplied by the solar collector network, kW
Q_i	Thermal load of hot stream i, kW
Q_j	Thermal load of cold stream j, kW
Q_s	Thermal load provided by a line of n collectors connected in series, Kw
SCN	Solar collector network
STE	Solar thermal energy
T_o	Collector outlet temperature n, °C
T_{inlet}	Current inlet temperature, °C
T_{outlet}	Current outlet temperature, °C
T_o^{n-1}	Collector outlet temperature n-1, °C
t	Total process supply time, h
ΔT	Temperature difference, °C
ΔT_{LMTD}	Logarithmic mean temperature difference, °C
ΔT_{LMTDk}	Logarithmic mean temperature difference of the interval, °C
ΔT_{min}	Minimum temperature difference, °C
$\Delta T_{min\ optimum}$	Minimum optimum temperature difference, °C
$\Delta T_{min,th}$	Minimum solar thermal temperature difference, °C
ΔT_{TTS}	Temperature variation in the thermal storage system, °C
U	Heat transfer global coefficient, kW/m^2°C
V_{TSS}	Thermal storage system volume, m^3
W	Width of solar collector, m
Greek letters	
η_{TSS}	Thermal storage system efficiency, dimensionless
ρ	Density of the working thermal fluid, kg/m^3
Constants	
a	Cost constant related to the materials of construction of the heat exchanger, 26600
a'	Cost constant for the storage tank type, 5800
b	Cost constant related to the operating pressure of the heat exchanger, 6500
b'	Cost constant for the storage tank, 1600
c	Cost constant related to the type of heat exchanger, 0.9
c'	Cost constant for the storage tank, 0.7

References

[1] Karki S, Haapala KR, Fronk BM. Technical and economic feasibility of solar flat-plate collector thermal energy systems for small and medium manufacturers. Appl Energy 2019;254:113649. https://doi.org/10.1016/j.apenergy.2019.113649.

[2] IEA - International Energy Agency. Renewable energy for industry. 2017. Access Date: https://prod.iea.org/reports/renewable-energy-for-industry. [Accessed 24 December 2020].

[3] IEA - International Energy Agency. Solar heating and cooling programme, solar heat worldwide. 2019. 2019, https://www.iea-shc.org/Data/Sites/1/publications/Solar-Heat-Worldwide-2019.pdf. [Accessed 24 December 2020].

[4] Farjana SH, Huda N, Mahmud MAP, Saidur R. Solar industrial process heating systems in operation – current SHIP plants and prospects in Australia. Renew Sustain Energy Rev 2018;91:409–19. https://doi.org/10.1016/j.rser.2018.03.105.

[5] Sharma AK, Sharma C, Mullick SC. Solar industrial process heating: a review. Renew Sustain Energy Rev 2017;78:124–37. https://doi.org/10.1016/j.rser.2017.04.079.

[6] Klemes JJ, Varbanov PS, Walmsley TG, Jia X. New directions in the implementation of pinch methodology (PM). Renew Sustain Energy Rev 2018;98:439–68. https://doi.org/10.1016/j.rser.2018.09.030.

[7] Atkins MJ, Walmsley MRW, Morrison AS. Integration of solar thermal for improved energy efficiency in low-temperature-pinch industrial processes. Energy 2010;35:1867–73. https://doi.org/10.1016/j.energy.2009.06.039.

[8] Nemet A, Kravanja Z, Klemeš JJ. Integration of solar thermal energy into processes with heat demand. Clean Technol Environ Policy 2012;14:453–63. https://doi.org/10.1007/s10098-012-0457-6.

[9] Quijera JA, González-Alriols M, Labidi J. Integration of a solar thermal system in canned fish factory. Appl Therm Eng 2014;70:1062–72. https://doi.org/10.1016/j.applthermaleng.2014.04.012.

[10] Eiholzer T, Olsen D, Hoffmann D, Sturm B, Wellig B. Integration of a solar thermal system in a medium-sized brewery using pinch analysis: methodology and case study. Appl Therm Eng 2017;113:1558–68. https://doi.org/10.1016/j.applthermaleng.2016.09.124.

[11] Baniassadi A, Momen M, Amidpour M. A new method for optimization of solar heat integration and solar fraction targeting in low temperature process industries. Energy 2015;90:1674–81. https://doi.org/10.1016/j.energy.2015.06.128.

[12] Walmsley TG, Walmsley MRW, Tarighaleslami AH. Integration options for solar thermal with low temperature industrial heat recovery loops. Energy 2015;90:113–21. https://doi.org/10.1016/j.energy.2015.05.080.

[13] Abdelhady F, Bamufleh H, El-Halwagi MM, Ponce-Ortega JM. Optimal design and integration of solar thermal collection, storage, and dispatch with process cogeneration systems. Chem Eng Sci 2015;136:158–67. https://doi.org/10.1016/j.ces.2015.04.043.

[14] Allouhi A, Agrouaz Y, Amine MB, Rehmand S, Buker MS, Kousksou T, Jamil A, Benbassou A. Design optimization of a multi-temperature solar thermal heating system for an industrial process. Appl Energy 2017;206:382–92. https://doi.org/10.1016/j.apenergy.2017.08.196.

[15] Velázquez-Torres D. Diseño de sistemas de suministro de energía térmica para procesos industriales asistidos con energía solar de baja temperatura. University of Guanajuato, M.S; 2020. Ch.E. dissertation. http://www.repositorio.ugto.mx/handle/20.500.12059/2206.

[16] Solar heat for industrial processes technology brief. International Renewable Energy Agency (IRENA); 2015. irena.org/publications/2015/Jan/Solar-Heat-for-Industrial-Processes. [Accessed 20 December 2020]. accessed.

[17] Martínez-Rodríguez G, Fuentes-Silva AL, Lizárraga-Morazán JR, Picón-Núñez M. Incorporating the concept of flexible operation in the design of solar

(continued on next page)

collector fields for industrial applications. Energies 2019;12:1–20. https://doi.org/10.3390/en12030570. 570.

[18] Fuentes-Silva AL, Velázquez-Torres D, Picón-Núñez M, Martínez-Rodríguez G. Solar thermal integration with and without energy storage: the cases of bioethanol and a dairy plant. Chem Eng Trans 2020;81:493–8. https://doi.org/10.3303/CET2081083.

[19] Wahed A, Bieri M, Kui TK, Reindl T. Levelized cost of solar thermal system for process heating applications in the tropics. In: Sayigh A, editor. Transition towards 100% renewable energy. Innovative renewable energy. Cham: Springer; 2018. https://doi.org/10.1007/978-3-319-69844-1_40.

[20] Tian Z, Perers B, Furbo S. Thermo-economic optimization of a hybrid solar district heating plant with flat plate collectors and parabolic trough collectors in series. Energy Convers Manag 2018;165:92–101. https://doi.org/10.1016/j.enconman.2018.03.034.

[21] Ghazouani M, Bouya M, Benaissa M, Anoune K, Ghazi M. Thermal energy management optimization of solar thermal energy system based on small parabolic trough collectors for bitumen maintaining on heat process. Sol Energy 2020;211:1403–21. https://doi.org/10.1016/j.solener.2020.10.074.

[22] Čuček L, Klemeš JJ, Kravanja Z. Overview of environmental footprints. In: Klemeš JJ, editor. Assessing and measuring environmental impact and sustainability. Oxford: Butterworth-Heinemann of Elsevier; 2015. p. 131–93.

[23] Arnaoutakis N, Souliotis M, Papaefthimiou S. Comparative experimental Life Cycle Assessment of two commercial solar thermal devices for domestic applications. Renew Energy 2017;111:187–200. https://doi.org/10.1016/j.renene.2017.04.008.

[24] Bogdanov D, Gulagi A, Fasihi M, Breyer C. Full energy sector transition towards 100% renewable energy supply: integrating power, heat, transport, and industry sectors including desalination. Appl Energy 2020:116273. https://doi.org/10.1016/j.apenergy.2020.116273.

[25] Sorknæs P, Østergaard PA, Thellufsen JZ, Lund H, Nielsen S, Djørup S, Sperling K. The benefits of 4th generation district heating in a 100% renewable energy system. Energy 2020;213:119030. https://doi.org/10.1016/j.energy.2020.119030.

[26] Linnhoff B. Introduction to Pinch technology linnhoff march. 1998. https://www.ou.edu/class/che-design/a-design/Introduction%20to%20Pinch%20Technology-LinhoffMarch.pdf.

[27] Budak N, Yucel HI, Yildiz C. Thermal performance enhancement of flat-plate solar collector by means of three different nanofluids. Therm Sci Eng Prog 2018:55–65. https://doi.org/10.1016/j.tsep.2018.07.005.

[28] Varbanov PS, Fodor Z, Klemeš JJ. Total Site targeting with process specific minimum temperature difference (ΔTmin). Energy 2012;44(1):20–8. https://doi.org/10.1016/j.energy.2011.12.025.

[29] Jiménez-Gutiérrez A. Diseño de procesos en ingeniería química. first ed. Barcelona: Editorial Reverté S. A.; 2003.

[30] Smith R. Chemical process design and integration. John Wiley & Sons, Ltd.; 2005.

[31] Lizárraga-Morazán JR, Martínez-Rodríguez G, Fuentes-Silva AL, Picón-Núñez M. Selection of solar collector network design for industrial applications subject to economic and operation criteria. EEG-EMG 2020. https://doi.org/10.1177/0958305X20927375.

[32] Yang P, Liu LL, Du J, Li JL, Meng QW. Heat exchanger network synthesis for batch processes by involving heat storages with cost targets. Appl Therm Eng 2014;70. https://doi.org/10.1016/j.applthermaleng.2014.05.041. 1276 - 128.

[33] Towler G, Sinnott R. Chemical engineering design. second ed. Oxford: Butterworth-Heinemann/Elsevier; 2013. www.academia.edu/25282800/Chemical_Engineering_Design_Principles_Practicet_and_Economics_of_Plant_and_Process_Design_Second_Edition.

[34] Quijera JA, González-Alriols M, Labidi J. Integration of a solar thermal system in a dairy process. Renew Energy 2011;36:1843–53. https://doi.org/10.1016/j.renene.2010.11.029.

[35] Oseguera-Villaseñor I. Reduction of the fossil fuel consumption to generate the required heat for the dehydration and purification of anhydrous bioethanol by means of solar energy. University of Guanajuato, M.S; 2016. Ch.E. dissertation. http://repositorio.ugto.mx/handle/20.500.12059/2139.

[36] Wallerand AS, Kermani M, Voillat R, Kantor I, Maréchal F. Optimal design of solar assisted industrial processes considering heat pumping: case study of a dairy. Renew Energy 2018;128:565–85. https://doi.org/10.1016/j.renene.2017.07.027.